Applied Surface Science 428 (2018) 54–60

Contents lists available at ScienceDirect

Applied Surface Science

journal homepage: www.elsevier.com/locate/apsusc

Full Length Article

Microwave absorption enhancement and dual-nonlinear magnetic resonance of ultra small nickel with quasi-one-dimensional nanostructure

Wei Xu [a], Ya-Fei Pan [a], Wei Wei [b], Guang-Sheng Wang [a,b,*], Peng Qu [b,*]

[a] Key Laboratory of Bio-Inspired Smart Interfacial Science and Technology of Ministry of Education, School of Chemistry, Beihang University, Beijing 100191, PR China

[b] Henan Key Laboratory of Biomolecular Recognition and Sensing,School of Chemistry and Chemical Engineering, Shangqiu Normal University, Shangqiu 476000, PR China

ARTICLE INFO

Article history:
Received 13 June 2017
Received in revised form 4 September 2017
Accepted 8 September 2017
Available online 9 September 2017

Keywords:
Quasi-one-dimensional structure
Ni nanochains
Microwave absorption
Magnetic loss
Low concentration

ABSTRACT

Quasi-one-dimensional (Q1D)nickel nanostructures were prepared by a facial wet chemical process, and then the nickel chains/polyvinylidene fluoride (PVDF) composites were fabricated using the hot-molding procedure. Both the complex permittivity and permeability of the Ni/PVDF composites could be artificially adjusted by changing the nickel proportions, which contribute to enhancing the microwave absorption. An excellent reflection loss (RL) of −42.08 dB at 7.4 GHz with a low filler loading(20 wt%)and effective bandwidth (RL <− 10 dB) of 10.7 GHz in the thickness range of 2–5 mm was obtained, which is expected that Ni/PVDF nanocomposites can be used as a novel and highly efficient microwave absorbers.

1. Introduction

Recently, due to the tremendous utilization of electronic devices in commercial and military fields, electromagnetic (EM) pollution has become one of the major environmental pollution, not only causing electro-magnetic interference with electronic devices but also resulting in negative effective to human health [1–3]. To solve this pollution, many researchers have been devoted enormous attention to effective microwave-absorbing materials with strong EM wave absorption capacity, broad absorption frequency, low density, excellent mechanical strength and high thermal stability [4]. Therefore, a variety of microwave absorption materials, such as carbon materials [5], graphene-based materials [6–8], semiconductor nanomaterials [9,10], metallic magnets [11], ferrites [12] and their hybrids [13–16], have been prepared successfully and displayed good microwave absorption performances. However, in some case, their drawbacks, such as large filler content, complex formation process, low yield or narrow absorption bandwidth, have severely restricted their use in practical applications. Among all the candidates for the purpose of microwave attenuation, representative metallic magnetic materials still have its fascinating advantages in some ways. For examples, Wen et al. [17] synthesized a series of cobalt particles through a liquid reduction process and the maximum absorption reflection loss can reach as high as −48.03 dB at 13.61 GHz. Yang et al. [18] milled commercially available α-Fe powders under controlled conditions to fabricate the flake-shaped Fe/epoxy composite absorbers. The best absorption performance is obtained, with the maximum absorption of −42.9 dB at 7.84 GHz. Han et al. [19] reported the preparation of ultra small Ni nanoparticles and Ni/polyaniline composites with different concentrations. The optimal RL value of composites can reach −22.98 dB at 17.8 GHz at a thin thickness of 1.0 mm.

Previous reports on various morphologies of microwave absorbers unit indicate that the well defined shape and controlled granularity of the absorber make it possible to control the microwave properties including high frequency permeability and resonance behaviors [11,20]. According to recent researches, quasi-one-dimensional materials such as MnO_2 nanowires [21], $NiCoO_4$ nanofibrous [22], carbon nanotubes [23,24] and so on stepped onto the platform of wave-absorbing materials and exhibited outstanding properties. As mentioned above, single-chain magnets with quasi-one-dimensional morphology are of great potential [25,26] as microwave absorbers because of their unique geometry and tun-

* Corresponding authors.
E-mail addresses: wanggsh@ustc.edu.cn (G.-S. Wang), qupeng0212@163.com (P. Qu).

http://dx.doi.org/10.1016/j.apsusc.2017.09.052
0169-4332/

able electromagnetic parameters. Their unique geometry with high aspect ratio leads to the higher coercivity, which are favorable for microwave absorption enhancement. For another hand, tunable electromagnetic parameters can realize good impedance match, which is a key to obtain superior microwave absorber.

As a candidate for microwave absorption, nickel has aroused extensively interest in the field of microwave absorption due to its large saturation magnetization and high Snoek's limit at high frequency band [27]. For example, Ni particles [19], core-shell microspheres with Ni cores [28–31], and nickel alloys [32–34] have all been reported to show good properties as EM wave absorbers. However, as far as we know, there are rare reports concerning Q1D Ni nanochains applied as electromagnetic-wave-absorbing materials [35]. Here, we report a facile, wet chemical method to synthesis Ni nanochains and the structures, the magnetic and microwave absorption properties were systematically studied. It was demonstrated that the content of fillers, as well as the type of matrix has a profound effect on the dielectric behavior and magnetic loss of absorbers, which in turn could influence their microwave attenuation behavior. A relative lower concentration of Ni nanochains in composites led to an outstanding microwave absorption property, which can meet the requirement of a light-weight characteristic. Specifically, when the Ni nanochains content reached certain critical levels, there was superior microwave absorption performance could be realized. Moreover, the mechanism of microwave absorption has been discussed in detail.

2. Experimental section

2.1. Preparation of nanochain-like nickel products

All the reagents were analytical grade and used as purchased without further purification. The nanochain-like Ni was prepared in a wet chemical process developed by Wei Zhou et al. Detailed experimental procedures are described in the following:quantities of 0.119 g of $NiCl_2{\cdot}6H_2O$ and 0.333 g of polyvinyl pyrrolidone (PVP; average M_W, 58 000) were added into 100 mL of the solvent ethylene glycol (EG) with vigorous stirring at room temperature for 2.5 h to form a light green transparent solution. Next, 0.265 mL of the hydrazine monohydrate liquid (80%) was added drop by drop, with continuing stirring from 1 to 2 h. Afterward, the solution was heated to 196 °C in a heating jacket and was refluxed for 3 h. Subsequently, the obtained precipitate was washed with ethanol several times and then centrifugated and dried in an oven at 60 °C.

2.2. Preparation of Ni/PVDF nanocomposites

The desired amount of poly(vinylidene fluoride)(PVDF) was dispersed in 25 mL of *N,N*-dimethylformamide (DMF) on a magnetic stirrer at room temperature for 30 min. Various contents of Ni nanochains were added while the solution became transparent. After ultrasonication for 10 min, the mixture was poured onto a glass plate to form a thin film, then dried at 80 °C for 3 h. The film was pressed into toroidal-shaped sample (Φ_{out} = 7.00 mm and Φ_{in} = 3.04 mm) by hot-pressing at 210 °C under 5 MPa.

2.3. Measurement of microwave absorption of nanocomposites

To measure the microwave absorption properties of nanocomposites, the samples were prepared by uniformly mixing in paraffin or PVDF matrix in different mass proportions andpressed into a compact cylindrical shape (Φ_{out} = 7.00 mm and Φ_{in} = 3.04 mm). The electromagnetics parameters were measured with the coaxial wire method by an Agilent N5224A vector network analyzer in the range of 2–18 GHz.

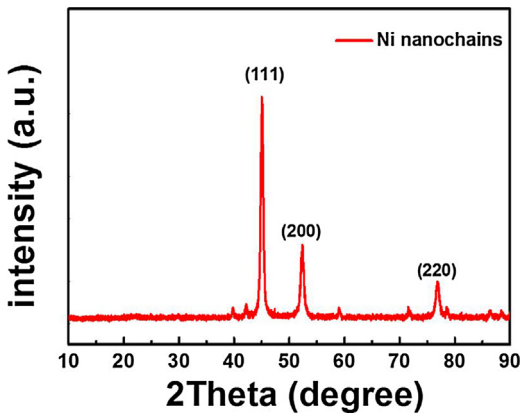

Fig 1. XRD patterns of the as-synthesized Ni nanochains.

2.4. Characterization

Powder X-ray diffraction (XRD) patternswere recorded using a Rigaku Dmax2200 X-ray diffractometer with Cu Kα radiation (λ = 1.5416 Å) for phase analysis. The morphologies and sizes of the Ni nanochains were characterized by scanning electron microscopy (SEM, JEOL JSM-7001F) and transmission electron microscopy (TEM, JEOL JEM-2010). The samples were prepared by dispersing in ethanol anddropping onto a copper grid supported by carbon films. Magnetic properties of thesamples were measured at room temperature using a Lakeshore Vibrating Sample Magnetometer (VSM, Riken Denshi Co. Ltd, Japan).

3. Results and discussion

3.1. Characterization and formation processof nickel chains

The phase information of as-synthesized sample was examined by powder X-ray diffraction (XRD). Fig. 1 shows the XRD patterns of a typical Ni nanochains sample without any impurities. The sharp diffraction peaks located at 44.5°, 51.8° and 76.7° corresponding tothe (111), (200) and (220) planes, respectively, and are well matched with the standard metallic face-centered cubic (fcc) structure (JCPDS no. 04-0850). To investigate the microstructure and morphology of the products, SEM, TEM and HRTEM studies were conducted. Fig. 2a and bare the representative scanning electron microscopy (SEM) images showing the quasi-one-dimensional chain-like structures where the observed nanochains has an outer diameter of approximately 30 nm and length up to 300 μm. It also can be seen that the as-prepared samples are uniform and axially aligned, aggregating to form irregularly cross-linked networks. Shown in Fig. 2c, the TEM image further reveals the chain-like structure with a rough surface. The selected area electron diffraction (SAED) pattern (inset in Fig. 2c) prove single-crystal structure of nickel. A high-resolution TEM image (Fig. 2d) shows the crystal planes of $(111)_{Ni}$ with a lattice spacing of 0.203 nm, also indicating a single-crystal nature.

The formation of quasi-one-dimensional chain-like structures could be explained based on the reaction conditions [36]. In the systems, $N_2H_4{\cdot}H_2O$ acts both as a ligandand a reducing agent while PVP molecules behaved like soft-templates during the reaction. In the solution, Ni^{2+}reacted with hydrazine to form $Ni[(N_2H_4)_3]^{2+}$ and the complex converted to Ni particles through homogeneous nucleation when the temperature rises to the boiling point of EG. These poly disperse particles had a tendency to undergo agglomeration and assembled into chains on account of the magnetic dipole–dipole interaction and the template effects of PVP.

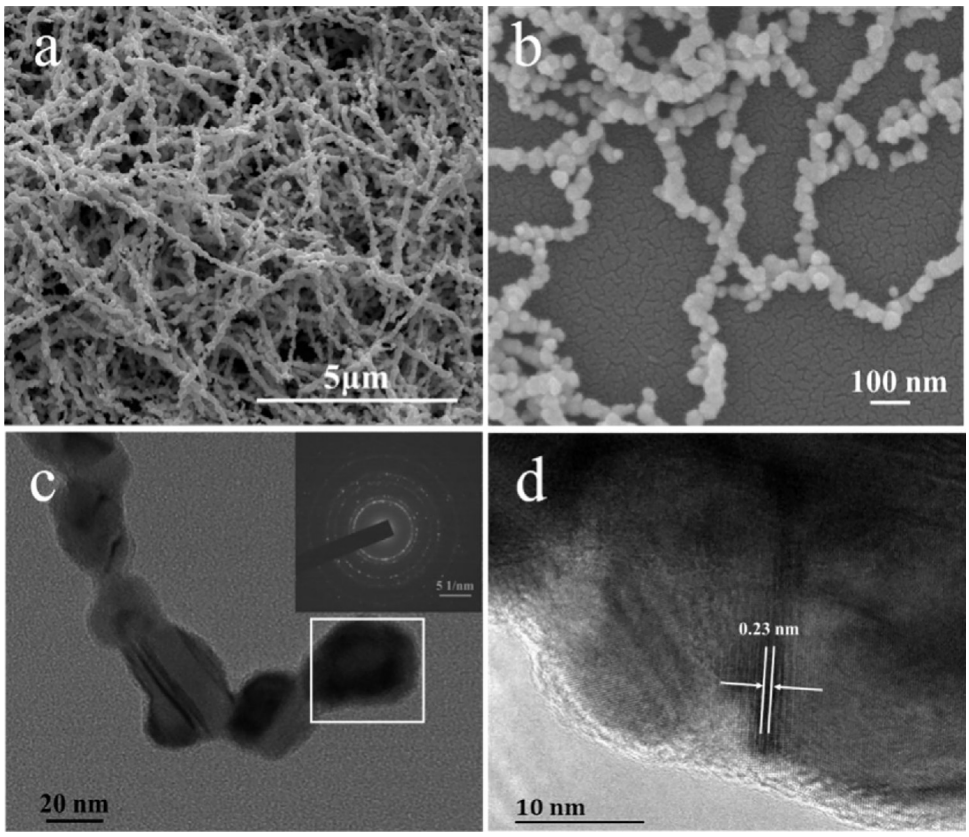

Fig. 2. (a, b) SEM images of the as-prepared nickel nanochains; (c) TEM image and SAED pattern (inset) of the nickel nanochains; (d) high resolution TEM image.

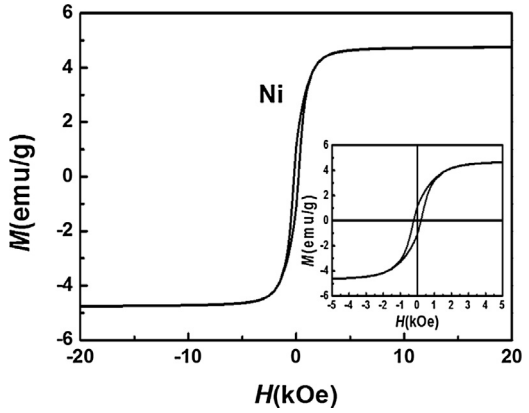

Fig. 3. Magnetization hysteresis loop of the Ni nanochains measured at room temperature.

As shown in Fig. 3, the magnetic hysteresis loops (M-H loops) of the nickel chainswere characterized at room temperature.Its values of saturation magnetization (M_s), remanent magnetization (M_r) and coercivity (H_c) are9.95 emu/g, 2.13 emu/g, and 200 O_e, respectively. Compared with other reports [20], the reduction in the M_s for ultrafine nanochains is usually ascribed to a decrease in the crystallinity and the surface encapsulation effect of the PVP. Compare with other shaped nickel, the H_c of nickel nanochain is significantly higher [35]. It is well known that the coercivity mainly depends on the various kinds of anisotropy such as magneto crystalline anisotropy andthe domain size of the magnetic particles, which is a key factor to determine microwave absorption performance of materials.

3.2. Electromagnetic and microwave absorption properties

In order to study the microwave absorption properties of samples, different proportions of Ni powders were mixed with PVDF or paraffin toform composites by a simple hot-pressing process, and the cross-sectional SEM image ofthe Ni/PVDF nanocomposite is shown in Fig. S1, revealing the uniform dispersion and intact structures of Ni nanochains in the polymer. According to the transmit line theory, the reflection loss (RL) of absorbing materials can be calculated using the electromagnetic parameters (relative complex permeability and permittivity) at a given frequency and different thickness layers. The reflection loss is related to Z_{in}as [37,38]:

$$RL = 20\log\left|\frac{z_{in}-1}{Z_{in}+1}\right| \quad (1)$$

where normalized input characteristic impedance (Z_{in}) is calculated as:

$$Z_{in} = \sqrt{\frac{\mu_r}{\varepsilon_r}}\tanh\left[j\left(\frac{2f\pi d}{c}\right)\sqrt{\mu_r\varepsilon_r}\right] \quad (2)$$

ε_r and μ_r are the complex permittivity and permeability of the composite absorber, respectively; f is the frequency; d is the thickness of the absorber, and c is the velocity of light in free space.

Fig. 4a presents the calculated reflection loss of the four samples at a thickness of 3 mm according to Eqs. (1) and (2). With an increasing content of nickel nanochains, the maximum RL values of Ni/PVDF composites increase initially and then decrease, shifting to a lower-frequency region meanwhile. It indicates that the frequency and bandwidth of microwave attenuation can be tuned by controlling the content of nickel nanochains. Furthermore, we can clearly see that the Ni/PVDF composites get enhanced significantly compared with the Ni/wax composites at the same loading amount. Concerning the wave-transparent property of paraffin

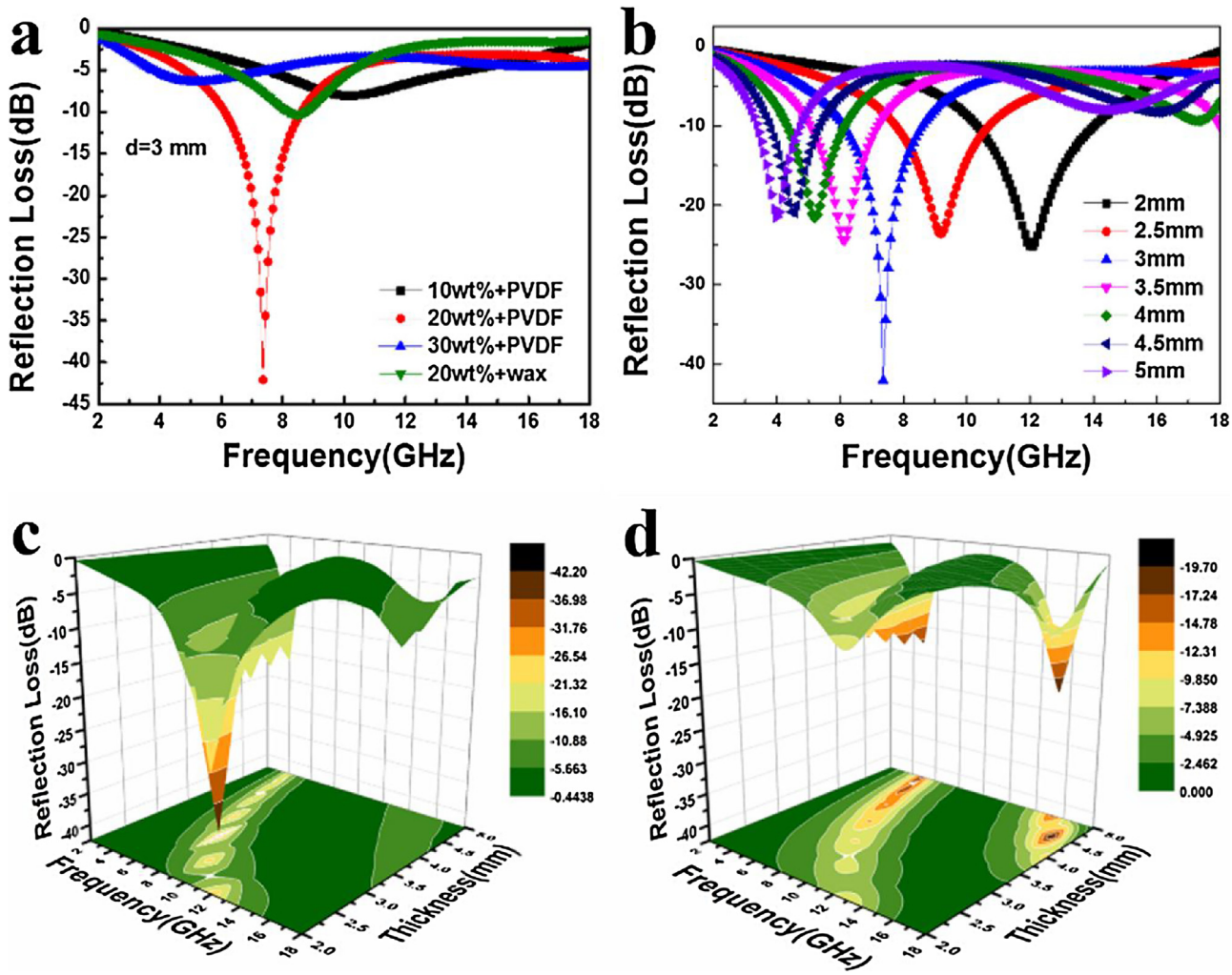

Fig. 4. Reflection loss of (a) the four samples with a thickness of 3 mm in the measuring range; (b) the 20 wt% filler proportion Ni/PVDF composites with a thickness range of 2–5 mm; (c) and (d) three-dimensional representations of the RL value of the 20 wt% filler proportion Ni/PVDF and Ni/wax composites.

matrix, paraffin-based composites often exhibit the pure fillers microwave absorption performances. Nevertheless, as PVDF is a typical dielectric material, the synergetic effect between Ni and PVDF would occur. It can be deduced that the synergetic effect in Ni/PVDF composites could enhance its microwave absorption ability. Fig. 4b shows the calculated theoretical RLs of Ni/PVDF at different thicknesses (2–5 mm) with 20 wt% proportion and the strongest RLvalue of the composites reaches −42.08 dB at 7.4 GHz with a matching thickness of 3 mm, and the effective absorption bandwidth (RL values lower than −10 dB) covers from 6.1 to 8.6 GHz. Note that the maximum RLs of composites shift toward lower frequency with the increasing thickness, corresponding to the quarter-wave length criteria model [39]:

$$t_m = n\lambda/4 = nc/4f_m(\varepsilon_r\mu_r)^{1/2} \quad (3)$$

where c is the velocity of light in vacuum, f_m is the peak frequency, t_m is the thickness of the sample, ε_r and μ_r are the relative complex permeability and permittivity at f_m, respectively. On the basis of Eq. (3), it is not hard to draw a conclusion that the peak frequency is in inverse proportion of the thickness of the absorber, and the higher ε_r and μ_r will result in a lower peak frequency under the same thickness.

To further demonstrate the microwave absorption properties more vividly, 3D image maps of the reflection loss of Ni/PVDF and Ni/wax nanocomposites with the same loading of 20 wt% are also shown in Fig. 4c and d. It can be observed that Ni/PVDF exhibit superior microwave absorption performance in both the value of RL and the bandwidth of absorption in comparison with Ni/wax nanocomposites, confirming a significantly enhanced effect of PVDF again. Meanwhile, in the RLs curves of Ni/wax composites, two peaks would be observed when the thickness reaches a certain value, and the peaks values are −19.6 dB at 16.7 GHz and −16.7 dB at 5.44 GHz with a thickness of 4 mm, respectively (Fig. 4d). The Ni/PVDF composite with a proportion of 10 wt% and 30 wt% are also shown in Fig. S2.

To investigate the possible mechanisms and effects to the enhancement of microwave absorption, the frequency dependence of electromagnetic parameters including complex permittivity real part ε', permittivity imaginary part ε'', permeability real part μ', and permeability imaginary part μ'' of all samples were measured (Fig. 5). As shown in Fig. 5a, for the Ni/PVDF nanocomposites, the real part (ε') of the permittivity connected with the ability to store EM energy increases with the increasing ratio of nickel nanochains, and shows similar decreasing trends in the measuring frequency. The imaginary part (ε'') with different ratios does not change much and maintain small values in the whole measuring range, indicating that the contribution of dielectric loss to microwave absorption is rather limitedbut favorable for impedance matching (Fig. 5b). For the pure metallic Ni, the values of ε' and ε'' almost remain constant through the entire frequency range ($\varepsilon' = 10$ and $\varepsilon'' = 1$).

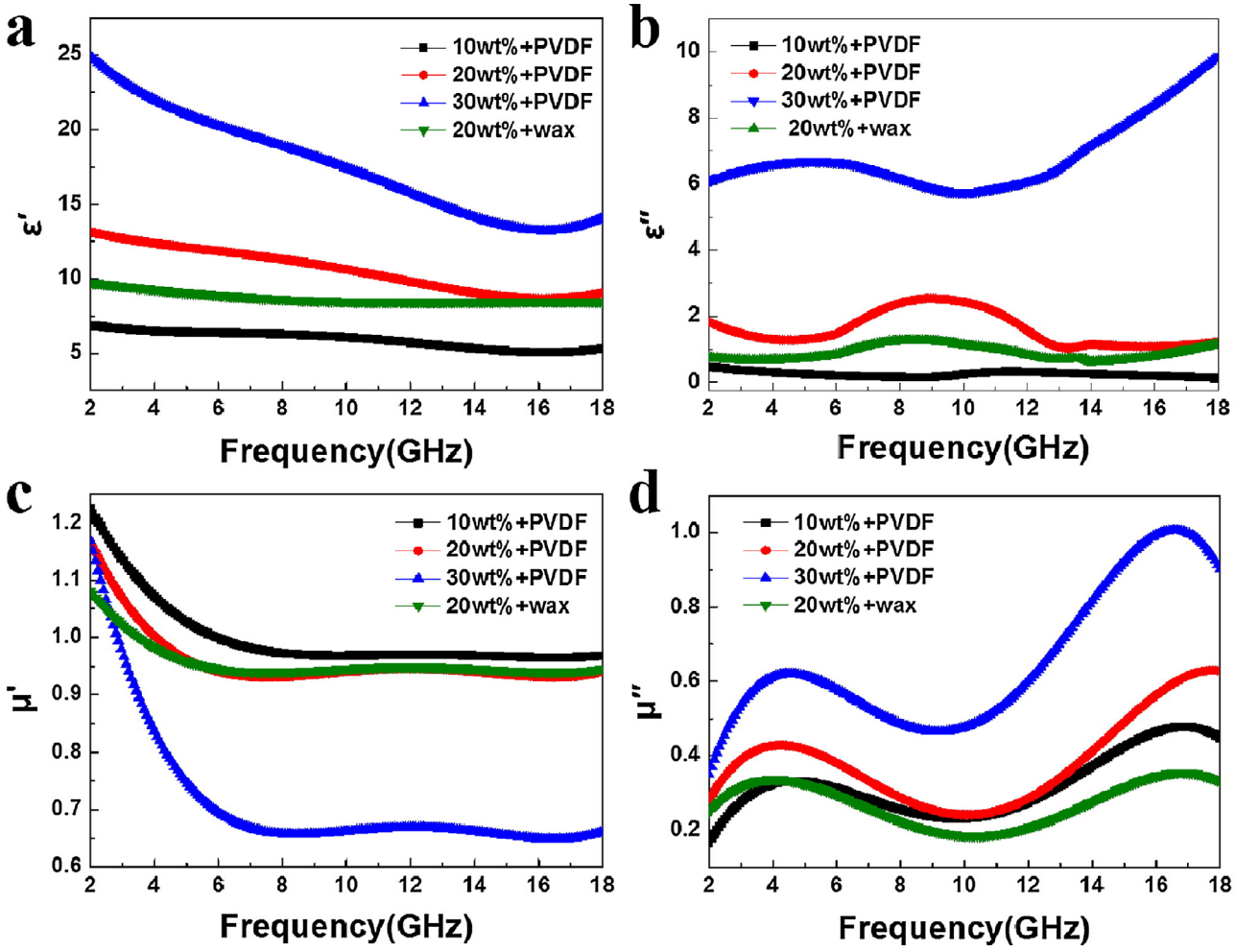

Fig. 5. Frequency dependence of real parts (a) and imaginary parts (b) of the complex permittivity, real parts (c) and imaginary parts (d) of the complex permeability.

The low values are mainly due to the weak conductivity of metallic nanochains. When the Ni compound with PVDF (at the same filler content of 20 wt%), the values of ε' and ε'' increases to 13.1 and 9.8, respectively. The enhancement of permittivity is quite reasonable because of the excellent polarization property of PVDF. Fig. 5c shows that the μ' values significantly reduce in the range of 2–6 GHz and then remain constant with minor fluctuations from 6 to 18 GHz, which could be ascribed to the relaxation of magnetic moments procession other than the magnetic hysteresis [40]. For the imaginary part (μ'') of the permeability (Fig. 5d), there are two distinct broad dual resonance peaks that can be observed at around 4–6 GHz and 16–18 GHz, respectively. The first resonance peak is mainly attributed to the natural resonance which expressed by the following formulas [41]:

$$2\pi f_r = rH_a \quad (4)$$

$$H_a = 4|K_1|/3\mu_0 M_s \quad (5)$$

Where r is the gyromagnetic ratio, H_a is the anisotropy energy, $|K_1|$ is the anisotropic coefficient, and the M_s is the saturated magnetization. According to the equation, the natural resonance frequencies depending on the effective anisotropy field do roughly agree well with the measured results, which may be associated with the small size effect and defects of nickel chains. The second resonance peak is probably derived from the exchange resonance which occurs usually at a higher frequency [28].

In theory, magnetic loss is implied by the imaginary part of permeability and may be attributed to hysteresis loss, domain wall resonance, exchange resonance, eddy current resonance, dimensional resonance and natural resonance [42,43]. For the Ni/PVDF composites, the hysteresis loss stemming from irreversible magnetization, as well as magnetic resonance owing to spin rotational component is almost negligible in a weak field [44]. Moreover, the domain wall resonance occurs only in the 1–100 MHz range [45], indicating that the dual resonance peaks at the frequencies of 2–18 GHz may be ascribed to the natural resonance and eddy current resonance [17]. To further demonstrate, the equation $C_0 =$

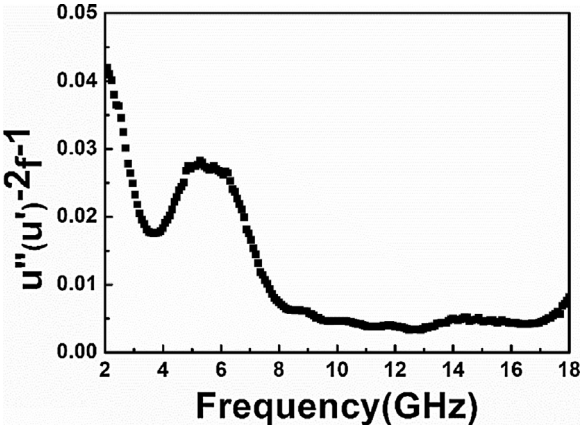

Fig. 6. The C_0-f curve of 20 wt% Ni/PVDF composite.

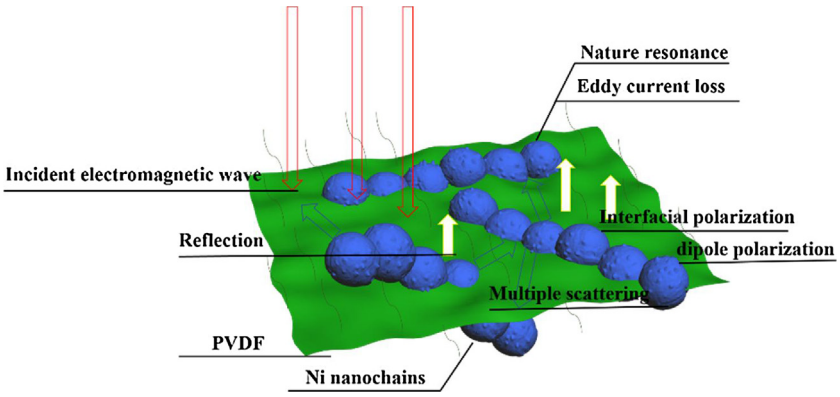

Fig. 7. Schematic illustration of possible microwave absorbing mechanisms of the Ni/PVDF composites.

$\mu''(\mu')^{-2}f^{-1} = 2/3\pi\mu_0 d^2\sigma$ [46,47] is introduced to evaluate eddy current loss. If the magnetic loss only results from eddy-current effect, the values of C_0 would be independent of the frequency and stay constant. As can be seen in Fig. 6, the value of the C_0 fluctuates in the range of 2–10 GHz and remains approximately constant from 10 to 18 GHz, indicating that eddy current loss has a great effect for the microwave energy dissipation. Generally, for most samples, the eddy current loss mainly appeared in the high frequency region (>10 GHz), which verifying the validity of our vision [40]. Hence, the magnetic loss in the measured frequency range is attributed to natural resonance, exchange resonance and eddy current resonance.

Based on the comprehensive analysis of the above EM parameters, we can draw a conclusion that the good EM absorption performances may be originated from some factors, as depicted in Fig. 7. Firstly, the tuned EM parameters lead to a good impedance matching behavior between the material and free space, which makes a large contribution to the significant improvement of microwave attenuation [48]. Secondly, such Q1D structures featuring special shape anisotropy, not only contribute to magnetic loss, but also provide more active sites for dissipating and scattering microwave. Thirdly, the interfacial polarization in this heterogeneous composite caused by the accumulation of charges at the interfaces and the formation of large dipoles on nickel nanochains could further improve the microwave absorption performance. Moreover, the interspace between the nickel nanochains and the matrix would induce multiple reflections and refractions, which results in more scattering dissipation. Overall, the enhanced microwave absorption capability of composites can be interpreted by good impedance match, strong magnetic loss including natural resonance and eddy current resonance, interfacial polarization, electronic dipole polarization and multiple scattering together.

4. Conclusions

In conclusion, we have successfully synthesized Q1D chain-like Ni nanomaterials by a facial wet chemical method and a series of Ni/PVDF and Ni/wax nanocomposites with different contents of Ni by a hot-molding procedure. By tuning the content of Ni, the nanocomposites exhibit an enhancement of microwave absorption even at the generally low concentration. The maximum reflection loss of 20 wt% Ni/PVDF nanocomposites can reach as high as −42.08 dB at 7.4 GHz with a matching thickness of 3 mm. The complex permittivity and permeability of the nanocomposites imply that natural resonance, eddy current resonance and interfacial polarization are the vital microwave loss mechanism. Furthermore, the effective absorption bandwidth was 10.7 GHz for thickness in the range of 2–5 mm, confirming that Ni/PVDF composites can act as a potential candidate in the field of microwave absorption, which is promising for solving the environmental pollution caused by microwave irradiation.

Acknowledgements

This project was supported by the National Nature Science Foundation of China (No.51472012), and Fundamental Research Funds for the Central Universities.

References

[1] S.I. Ohkoshi, S. Kuroki, S. Sakurai, K. Matsumoto, K. Sato, S. Sasaki, A millimeter-wave absorber based on gallium-substituted ε-Iron oxide nanomagnets, Angew. Chem. Int. Ed. 46 (2007) 8392–8395.
[2] Y. Lü, Y. Wang, H. Li, Y. Lin, Z. Jiang, Z. Xie, Q. Kuang, L. Zheng, MOF-derived porous Co/C nanocomposites with excellent electromagnetic wave absorption properties, ACS Appl. Mater. Interfaces 7 (2015) 13604–13611.
[3] A. Hirata, S. Matsuyama, T. Shiozawa, Temperature rises in the human eye exposed to EM waves in the frequency range 0.6–6 GHz, IEEE Trans. Electromagn. Compat. 42 (2000) 386–393.
[4] G.X. Tong, F.T. Liu, W.H. Wu, F.F. Du, J.G. Guan, Rambutan-like Ni/MWCNT heterostructures: easy synthesis formation mechanism, and controlled static magnetic and microwave electromagnetic characteristics, J. Mater. Chem. A 2 (2014) 7373–7382.
[5] X.F. Zhang, X.L. Dong, H. Huang, Y.Y. Liu, W.N. Wang, X.G. Zhu, B. Lv, J.P. Lei, Microwave absorption properties of the carbon-coated nickel nanocapsules, Appl. Phys. Lett. 89 (2006) 053115.
[6] Y. Zhang, Y. Huang, T.F. Zhang, H.C. Chang, P.S. Xiao, H.H. Chen, Z.Y. Huang, Y.S. Chen, Broadband and tunable high-performance microwave absorption of an ultralight and highly compressible graphene foam, Adv. Mater. 27 (2015) 2049.
[7] X.-J. Zhang, G.-S. Wang, Y.-Z. Wei, L. Guo, M.-S. Cao, Polymer-composite with high dielectric constant and enhanced absorption properties based on graphene–CuS nanocomposites and polyvinylidene fluoride, J. Mater. Chem. A 1 (2013) 12115–12122.
[8] B. Zhong, W. Liu, Y.L. Yu, L. Xia, J.L. Zhang, Z.F. Chai, G.W. Wen, Enhanced microwave absorption properties of graphite nanoflakes by coating hexagonal boron nitride nanocrystals, Appl. Surf. Sci. 420 (2017) 858–867.
[9] G.-S. Wang, Y.-Y. Wu, X.-J. Zhang, Y. Li, L. Guo, M.-S. Cao, Controllable synthesis of uniform ZnO nanorods and their enhanced dielectric and absorption properties, J. Mater. Chem. A 2 (2014) 8644–8651.
[10] S. He, G.-S. Wang, C. Lu, X. Luo, B. Wen, L. Guo, M.-S. Cao, Controllable fabrication of CuShierarchical nanostructures and their optical, photocatalytic, and wave absorption properties, Chempluschem 78 (2013) 250–258.
[11] F. Ma, Y. Qin, Y.-Z. Li, Enhanced microwave performance of cobalt nanoflakes with strong shape anisotropy, Appl. Phys. Lett. 96 (2010) 202507.
[12] J.T. Zhou, Z.J. Yao, T.T. Yao, Synthesis and electromagnetic property of $Li_{0.35}Zn_{0.3}Fe_{2.35}O_4$ grafted with polyaniline fibers, Appl. Surf. Sci. 420 (2017) 154–160.
[13] P.J. Liu, Z.J. Yao, J.T. Zhou, Z.H. Yang, L.B. Kong, Small magnetic Co-doped Ni Zn ferrite/graphene nanocomposites and their dual-region microwave absorption performance, J. Mater. Chem. C 4 (2016) 9738–9749.
[14] X. Wang, X. Huang, Z. Chen, X. Liao, C. Liu, B. Shi, Ferromagnetic hierarchical carbon nanofiber bundles derived from natural collagen fibers: truly lightweight and high-performance microwave absorption materials, J. Mater. Chem. C 3 (2015) 10146–10153.
[15] T. Wu, Y. Liu, X. Zeng, T.T. Cui, Y.T. Zhao, Y.N. Li, G.X. Tong, Facile hydrothermal synthesis of Fe_3O_4/C core-shell nanorings for efficient low-frequency microwave absorption, ACS Appl. Mater. Interfaces 8 (2016) 7370–7380.

[16] N. Li, G.W. Huang, Y.Q. Li, H.M. Xiao, Q.P. Feng, N. Hu, S.Y. Fu, Enhanced microwave absorption performance of coated carbon nanotubes by optimizing the Fe_3O_4 nanocoating structure, ACS Appl. Mater. Interfaces 9 (2017) 2973–2983.
[17] S.L. Wen, Y. Liu, X.C. Zhao, J.W. Cheng, H. Li, Synthesis dual-nonlinear magnetic resonance and microwave absorption properties of nanosheet hierarchical cobalt particles, Phys. Chem. Chem. Phys. 16 (2014) 18333–18340.
[18] R.-B. Yang, W.-F. Liang, S.-T. Choi, C.-K. Lin, Theeffects of size and shape of iron particles on the microwaveabsorbing properties of composite absorbers, IEEE Trans. Magn. 49 (2013) 4180–4183.
[19] D.D. Han, N.R. Xiao, H. Hu, B. Liu, G.X. Song, H. Yan, Ultrasmall superparamagnetic Ni nanoparticles embedded in polyaniline as a lightweight and thin microwave absorber, RSC Adv. 5 (2015) 66667–66673.
[20] P.W. Li, W.M. Chen, W. Liu, Z.A. Li, Y.M. Cui, A.P. Huang, R.M. Wang, C.P. Chen, Thermodynamic phase formation of morphology and size controlled Ni nanochains bytemperature and magnetic field, J. Phys. Chem. C 114 (2010) 7721–7726.
[21] W. Xu, G.C. Lv, X.B. Xing, X.-J. Zhang, G.-S. Wang, Fabrication of akhtenskite nanowires and their enhanced microwave absorption properties, Sci. Adv. Mater. 8 (2016) 966–971.
[22] J. Zhan, Y.L. Yao, C.F. Zhang, C.J. Li, Synthesis and microwave absorbing properties of quasi-one-dimensional mesoporous $NiCo_2O_4$ nanostructure, J. Alloys Compd. 585 (2014) 240–244.
[23] J.H. Zhou, J.P. He, G.X. Li, T. Wang, D. Sun, X.C. Ding, J.Q. Zhao, S.C. Wu, Direct incorporation of magnetic constituents within ordered mesoporous carbon-silica nanocomposites for highly efficient electromagnetic wave absorbers, J. Phys. Chem. C 114 (2010) 7611–7617.
[24] R.C. Che, L.-M. Peng, X.F. Duan, Q. Chen, X.L. Liang, Microwave absorption enhancement and complex permittivity and permeability of Fe encapsulated within carbon nanotubes, Adv. Mater. 16 (2004) 401–405.
[25] X. Zhan, H. Tang, Y. Du, A. Talbi, J. Zha, J. He, Facile preparation of Fe nanochains and their electromagnetic properties, RSC Adv. 3 (2013) 15966–15970.
[26] S.-Q. Lv, Y.-F. Pan, P.-B. Yang, G.-S. Wang, Hybrids of cobalt nanochains and polyvinylidenefluoride with enhanced microwave absorptionperformance, RSC Adv. 6 (2016) 55546–55551.
[27] J.-R. Liu, M. Itoh, T. Horikawa, K. Machida, S. Sugimoto, T. Maeda, Gigahertz range electromagnetic wave absorbers made of amorphous-carbon-based magnetic nanocomposites, J. Appl. Phys. 98 (2005) (054305-7).
[28] B. Zhao, G. Shao, B. Fan, W. Zhao, Y. Xie, R. Zhang, Facile preparation and enhanced microwaveabsorption properties of core-shell compositespheres composited of Ni cores and TiO_2shells, Phys. Chem. Chem. Phys. 17 (2015) 8802–8810.
[29] B. Zhao, G. Shao, B. Fan, W. Zhao, R. Zhang, Investigation of the electromagnetic absorptionproperties of Ni@$TiO_2$and Ni@SiO_2compositemicrospheres with core-shell structure, Phys. Chem. Chem. Phys. 17 (2014) 2531–2539.
[30] B. Lu, X.L. Dong, H. Huang, X.F. Zhang, X.G. Zhu, J.P. Lei, J.P. Sun, Microwave absorption properties of the core/shell-type iron and nickel nanoparticles, J. Magn. Magn. Mater. 320 (2008) 1106–1111.
[31] B. Zhao, X.Q. Guo, W.Y. Zhao, J.S. Deng, G. Shao, B.B. Fan, Z.Y. Bai, R. Zhang, Yolk-shell Ni@SnO_2 composites with a designable interspace to improve electromagnetic wave absorption properties, ACS Appl. Mater. Interfaces 8 (2016) 28917–28925.
[32] Q. Liu, X. Xu, W. Xia, R. Che, C. Chen, Q. Cao, J. He, Dependency of magnetic microwave absorption on surface architecture of $Co_{20}Ni_{80}$ hierarchical structures studied by electron holography, Nanoscale 7 (2015) 1736–1743.
[33] B. Zhao, W.Y. Zhao, G. Shao, B.B. Fan, R. Zhang, Morphology-control synthesis of a core-shell structured NiCu alloy withtunable electromagnetic-wave absorption capabilities, ACS Appl. Mater. Interfaces 7 (2015) 12951–12960.
[34] Q.H. Liu, Q. Cao, X.B. Zhao, H. Bi, C. Wang, D.S. Wu, R.C. Che, Insights into size-dominant magnetic microwave absorption properties of CoNimicroflowers via off-axis electron holography, ACS Appl. Mater. Interfaces 7 (2015) 4233–4240.
[35] J. Liu, M.-S. Cao, Q. Luo, H.-L. Shi, W.-Z. Wang, J. Yuan, Electromagnetic property and tunable microwave absorption of 3D nets from nickel chains at elevated temperature, ACS Appl. Mater. Interfaces 8 (2016) 22615–22622.
[36] C.-M. Liu, L. Guo, R.-M. Wang, Y. Deng, H.-B. Xu, S.H. Yang, Magnetic nanochains of metal formed by assembly of small nanoparticles, Chem. Commun. 23 (2004) 2726–2727.
[37] W.Z. Li, T. Qiu, L.L. Wang, S.S. Ren, J.R. Zhang, L.F. He, X.Y. Li, Preparation and electromagnetic properties of core/shell polystyrene@polypyrrole@nickel composite microspheres, ACS Appl. Mater. Interfaces 5 (2013) 883–891.
[38] W.C. Zhou, X.J. Hu, X.X. Bai, S.Y. Zhou, C.Y. Sun, J. Yan, P. Chen, Synthesis and electromagnetic microwave absorbing properties of core-shell Fe_3O_4-Poly(3, 4-ethylenedioxythiophene) microspheres, ACS Appl. Mater. Interfaces 3 (2011) 3839–3845.
[39] Y.B. Feng, T. Qiu, Preparation, characterization and microwave absorbing properties of FeNi alloy prepared by gas atomization method, J. Alloys Compd. 513 (2012) 455–459.
[40] Q.H. Liu, Q. Cao, H. Bi, C.Y. Liang, K.P. Yuan, W. She, Y.J. Yang, CoNi@SiO_2@TiO_2 and CoNi@Air@TiO_2microspheres with strong wideband microwave absorption, Adv. Mater. 28 (2015) 486–490.
[41] H.L. Lv, X.H. Liang, G.B. Ji, H.Q. Zhang, Y.W. Du, Porous Three-dimensional flower-like Co/CoO and its excellent electromagnetic absorption properties, ACS Appl. Mater. Interfaces 7 (2015) 9776–9783.
[42] P. Liu, H. Ying, Y. Jing, Y. Yang, Z. Yang, Construction of CuS nanoflakes vertically aligned on magnetically decorated graphene and their enhanced microwave absorption properties, ACS Appl. Mater. Interfaces 8 (2016) 5536–5546.
[43] F. Wen, H. Yi, L. Qiao, H. Zheng, D. Zhou, F. Li, Analyses on double resonance behavior in microwave magnetic permeability of multiwalled carbon nanotube composites containing Ni catalyst, Appl. Phys. Lett. 92 (2008) 1032.
[44] Z. Li, Y. Deng, B. Shen, W. Hu, Preparation and microwave absorption properties of Ni-Fe_3O_4, hollow spheres, J. Mater. Sci. Eng. B 164 (2009) 112–115.
[45] Y. Du, W. Liu, R. Qiang, Y. Wang, X. Han, J. Ma, P. Xu, Shell thickness-dependent microwave absorption of core-shell Fe_3O_4@C composites, ACS Appl. Mater. Interfaces 6 (2014) 12997–13006.
[46] C.-L. Zhu, M.-L. Zhang, Y.-J. Qiao, G. Xiao, F. Zhang, Y.-J. Chen, Fe_3O_4/TiO_2core/shell nanotubes: synthesis and magnetic and electromagnetic waveabsorption characteristics, J. Phys. Chem. C 114 (2010) 16229–16235.
[47] M.Z. Wu, Y.D. Zhang, S. Hui, T.D. Xiao, S.H. Ge, W.A. Hines, J.I. Budnick, G.W. Taylor, Microwave magnetic properties of $Co_{50}/(SiO_2)_{50}$ nanoparticles, Appl. Phys. Lett. 80 (2002) 4404.
[48] Z. Wang, Y. Zuo, Y. Yao, L. Xi, J. Du, J. Wang, D. Xue, Microwave absorption properties of amorphous iron nanostructures fabricated by a high-yield method, J. Phys. D: Appl. Phys. 46 (2013) 135002.